Journal of Zhejiang University SCIENCE A
ISSN 1673-565X (Print); ISSN 1862-1775 (Online)
www.zju.edu.cn/jzus; www.springerlink.com
E-mail: jzus@zju.edu.cn

Vibration analysis of maglev three-span continuous guideway considering control system

Yan-feng TENG[†], Nian-guan TENG[†‡], Xin-jian KOU

(*School of Naval Ocean, Architecture and Civil Engineering, Shanghai Jiao Tong University, Shanghai 200240, China*)

[†]E-mail: tyfsjtu@163.com; ngteng@sjtu.edu.cn

Received Apr. 20, 2007; revision accepted June 20, 2007; published online Nov. 10, 2007

Abstract: The dynamic interaction between maglev vehicle and three-span continuous guideway is discussed. With the consideration of control system, the dynamic interaction model has been developed. Numerical simulation has been performed to study dynamic characteristics of the guideway. The results show that bending rigidity, vehicle speed, span ratio and primary frequency all have important influences on the dynamic characteristics of the guideway and there is no distinct trend towards resonance vibration when $f_1/(v/l)$ equals 1.0. The definite way is to control impact coefficient and acceleration of the guideway. The conclusions can serve the design of high-speed maglev three-span continuous guideway.

Key words: Maglev transportation system, Three-span continuous guideway, Coupling dynamics, Feedback control, Numerical simulation

doi:10.1631/jzus.A071214 **Document code:** A **CLC number:** U441[+].4

INTRODUCTION

The maglev transportation system based on magnetically levitated vehicles is a high-speed ground transportation system which has been proposed to meet future requirements of intercity transportation. The Shanghai Maglev Transportation System built in 2003 is the first commercial high-speed maglev transportation system in the world, and its success will greatly promote the development of maglev transportation system in China.

In the past thirty years, research and study have been focusing on the areas of magnetic levitation and optimization of vehicle suspensions (Cai *et al.*, 1994). Recently maglev guideway has attracted more and more attention. The maglev guideway typically represents about one half of the cost so considerable efforts have been made to keep the guideway as small and light as possible. For the maglev transportation system, as the vehicle speed reaches to 500 km/h and the guideway is flexible enough to reduce the cost, the dynamic interaction between the vehicle and guideway will be more important and play a dominant role in the whole system.

According to the research and documents presented currently in the area of dynamic interaction between maglev vehicle and guideway, the achievements are mainly classified into two categories. One is to focus on the dynamic characteristics of vehicle and the improvements on control system for magnetic levitation (Nagurka, 1995; Wang, 1995; Cai and Chen, 1996; Wu *et al.*, 2000; Sinha and Pechev, 2004; Deng *et al.*, 2006; Wang and Li, 2007). In this category the control system is studied with different complicate control models. Its main objective is to study the principle of magnetic levitation and to improve the performance of the control system. The vibration of guideway is just considered as a disturbance to the control system, so the guideway model is always simple. The other is to focus on dynamic characteristics of guideway which dynamically interacts with the passing vehicles (Meisinger, 1991; Cai *et al.*, 1994;

‡ Corresponding author

* Project (No. 2005AA505440) supported by the Hi-Tech Research and Development Program (863) of China

Zhao and Zhai, 2002; Shi *et al.*, 2006; 2007). In this category the magnetic force is simplified as a group of concentrated forces or spring-dampers. Its main aim is to study the dynamic characteristics of the guideway and to offer certain requirements and specifications for guideway stiffness, weight and span length. Because the magnetic force between vehicle and guideway is distributed and controlled by the control system, this model cannot reflect the real working state of the system (Hong and Li, 2005).

With rapid development of high-speed maglev transportation system, it is inevitable to confront the problems of crossing rivers and main roads in city. In this aspect there are no ready-made techniques in German and Japan for reference. It is necessary to develop guideway with medium span length to meet these demands. Three-span continuous guideway is a good solution to this problem and has attracted more interests in practice. This paper is to discuss the problems about modeling vehicle/guideway dynamic interaction and to study the dynamic characteristics of three-span continuous guideway with different parameters. A Bernoulli-Euler beam equation is used to model the guideway. With consideration of the control system, the vehicle/guideway dynamic interaction model has been developed. Numerical simulation has been performed to study the dynamic characteristics of three-span continuous guideway. The results can serve the design of high-speed maglev three-span continuous guideway.

VEHICLE/GUIDEWAY DYNAMIC INTERACTION MODEL

Vehicle dynamic model

Based on the structure of TR06 maglev vehicle (Zhao and Zhai, 2002), a simplified vehicle model is shown in Fig.1. In this model, magnetic levitation system acted as the primary suspension instead of spring-dampers.

According to Newton's theory, equations of the vehicle motions are described as follows:

(1) Carbody Heave and Pitch

$$M_{\mathrm{c}}\ddot{y}_{\mathrm{c}}+\sum_{i=1}^{8}c_{\mathrm{s}}(\dot{y}_{\mathrm{su}i}-\dot{y}_{\mathrm{sb}i})+\sum_{i=1}^{8}k_{\mathrm{s}}(y_{\mathrm{su}i}-y_{\mathrm{sb}i})=0\,, \quad (1)$$

$$J_{\mathrm{c}}\ddot{\alpha}+\sum_{i=1}^{8}c_{\mathrm{s}}l_{si}(\dot{y}_{\mathrm{su}i}-\dot{y}_{\mathrm{sb}i})+\sum_{i=1}^{8}k_{\mathrm{s}}l_{si}(y_{\mathrm{su}i}-y_{\mathrm{sb}i})=0\,, \quad (2)$$

where M_{c} and J_{c} are the mass and the mass inertia of the carbody, k_{s} and c_{s} are the stiffness and the damping of secondary suspension, y_{c} and α are vertical displacement and the pitch angle of carbody, $y_{\mathrm{su}i}$ and $y_{\mathrm{sb}i}$ indicate the vertical displacement of the top and the bottom of the ith secondary spring-damper, l_{si} is the horizontal distance between the center of the carbody and the ith secondary spring-damper.

(2) Bogie Heave and Pitch

$$M_{\mathrm{b}}\ddot{y}_{\mathrm{b}j}-\sum_{i=2,j-1}^{2j}c_{\mathrm{s}}(\dot{y}_{\mathrm{su}i}-\dot{y}_{\mathrm{sb}i})-\sum_{i=2,j-1}^{2j}k_{\mathrm{s}}(y_{\mathrm{su}i}-y_{\mathrm{sb}i})+\sum_{k=1}^{4}f_{\mathrm{v}k}=0,\ j=1,2,3,4, \quad (3)$$

$$J_{\mathrm{b}}\ddot{\beta}_{\mathrm{b}j}+\sum_{i=2j-1}^{2j}c_{\mathrm{s}}l_{\mathrm{b}}(\dot{y}_{\mathrm{su}i}-\dot{y}_{\mathrm{sb}i})-\sum_{i=2j-1}^{2j}k_{\mathrm{s}}l_{\mathrm{b}}(y_{\mathrm{su}i}-y_{\mathrm{sb}i})+\sum_{k=1}^{4}f_{\mathrm{v}k}l_{\mathrm{p}k}=0,\quad j=1,2,3,4, \quad (4)$$

where M_{b} and J_{b} are the mass and the mass inertia of bogie, $y_{\mathrm{b}j}$ and β_j are vertical displacement and the pitch angle of jth bogie, l_{b} is the horizontal distance between the center of bogie and the secondary spring-damper, $l_{\mathrm{p}k}$ is the horizontal distance between the center of bogie and the kth magnetic levitation module installed under the jth bogie, $f_{\mathrm{v}k}$ is the magnetic force acting on the vehicle generated by the kth magnetic levitation module.

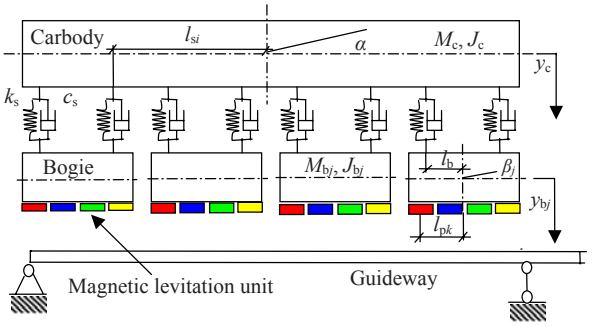

Fig.1 The vehicle model

Magnet model

The magnet system is shown in Fig.2 (Wang, 1995). The current in the constant current coil is constant and the resulting magnet force provides the lifting capability to balance the total weight in static equilibrium. The control current i in the control coils

is driven by control voltage u to maintain the air gap h at its nominal value.

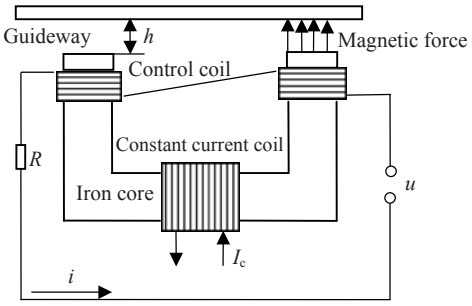

Fig.2 The magnet model

The attractive magnetic force f generated by the kth magnetic levitation unit can be represented as (Wang, 1995):

$$f=\frac{\mu_0 A_m}{4h^2}(N_c I_c+N_T i)^2. \quad (5)$$

From Kirchhoff's voltage law, the equation relating the control current with the control voltage can be expressed as (Wang, 1995):

$$u=Ri+\frac{\mu_0 A_m N_T^2}{2h}\frac{\mathrm{d}i}{\mathrm{d}t}-\frac{\mu_0 A_m N_T(N_c I_c+N_T i)}{2h^2}\frac{\mathrm{d}h}{\mathrm{d}t}, \quad (6)$$

where u is the control voltage; R is the resistance of the control coil; N_c and N_T are the numbers of turns in the constant current coil and the control coils, respectively; μ_0 is permeability of air; A_m is the face area of magnetic pole; dh/dt is air gap rate. The control current can be obtained by solving Eq.(6).

Controller model

The task of the control system is to dynamically regulate the control voltage which drives the magnet to adjust the magnetic force to maintain a nominal gap. Based on feedback signals from sensors, the controller can generate certain control voltage according to control algorithm. A PD (proportional plus derivative control) controller widely used in practice is adopted. The control algorithm is described as follows:

$$u=k_p[h(t)-h_0]+k_d h'(t), \quad (7)$$

where h_0 is the nominal value of $h(t)$; k_p and k_d are the parameters of PD control algorithm. $h(t)$ and dh/dt obtained from the sensors are sent to the controller as feedback signal.

Guideway model

The guideway model shown in Fig.3 consists of main span and side span. l_1 and l_2 is the length of side span and main span of the guideway, respectively. EI is the bending rigidity and m is the mass per unit length of the guideway.

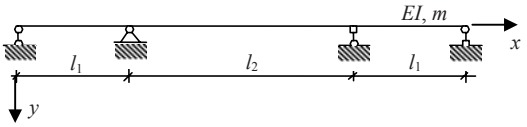

Fig.3 The guideway model

The mode shape of three-span continuous guideway $\phi(x)$, is divided into two groups: symmetrical mode shape $\phi_s(x)$ and asymmetrical mode shape $\phi_a(x)$. So the frequency equation shown in Eq.(8) includes two equations. Eq.(8a) corresponds to asymmetrical mode shape and Eq.(8b) corresponds to symmetrical mode shape.

$$\cot(\lambda l_1)-\mathrm{cth}(\lambda l_1)+\cot(\lambda l_1)-\mathrm{cth}(\lambda l_1)+(\sec(\lambda l_2)-\mathrm{sech}(\lambda l_2))=0, \quad (8a)$$

$$\cot(\lambda l_1)-\mathrm{cth}(\lambda l_1)+\cot(\lambda l_1)-\mathrm{cth}(\lambda l_1)-(\sec(\lambda l_2)-\mathrm{sech}(\lambda l_2))=0, \quad (8b)$$

where

$$\lambda=\sqrt[4]{m\omega^2/(EI)}. \quad (9)$$

After solving Eq.(8) the circular frequency ω can be obtained from Eq.(9).

The mode shapes of the guideway are expressed as follows:

when $x\in[0, l_1]$,

$$\phi(x)=\sin(\lambda x)\cdot\sec(\lambda l_1)-\sinh(\lambda x)\cdot\mathrm{sech}(\lambda l_1); \quad (10)$$

when $x\in[l_1, l_1+l_2]$, let $x_m=x-l_1$,

$$\phi_s(x_m)=\cos(\lambda x_m)-\cosh(\lambda x_m)-(\cos(\lambda l_2)+1)\cdot\sec(\lambda l_2)\cdot\sin(\lambda x_m)+(\cosh(\lambda l_2)+1)\cdot\mathrm{sech}(\lambda l_2)\cdot\sinh(\lambda x_m); \quad (11a)$$

$$\phi_a(x_m)=\cos(\lambda x_m)-\cosh(\lambda x_m)-(\cos(\lambda l_2)-1)\cdot\sec(\lambda l_2)\cdot\sin(\lambda x_m)+(\cosh(\lambda l_2)-1)\cdot\mathrm{sech}(\lambda l_2)\cdot\sinh(\lambda x_m); \quad (11b)$$

when $x\in[l_1+l_2, 2l_1+l_2]$, let $x_r=x-l_1-l_2$,

$$\phi_s(x_r)=-\cos(\lambda x_r)+\cosh(\lambda x_r)+(\cos(\lambda l_1)+1)\cdot\sec(\lambda l_1)\cdot\sin(\lambda x_r)-(\cosh(\lambda l_1)+1)\cdot\mathrm{sech}(\lambda l_1)\cdot\sinh(\lambda x_r); \quad (12a)$$

$$\phi_a(x_r)=\cos(\lambda x_r)-\cosh(\lambda x_r)-\cos(\lambda l_1)\cdot\sec(\lambda l_1)\cdot\sin(\lambda x_r)+\cosh(\lambda l_1)\cdot\operatorname{sech}(\lambda l_1)\cdot\sinh(\lambda x_r). \quad (12b)$$

A Bernoulli-Euler beam is assumed in the guideway model. The equation of vertical motion of the guideway subjected to arbitrary distributed load can be expressed as:

$$EI\frac{\partial^4 y}{\partial x^4}+C_s I\frac{\partial^5 y}{\partial t\partial x^4}+m\frac{\partial^2 y}{\partial t^2}+C(x)\frac{\partial y}{\partial t}=q(x,t), \quad (13)$$

where t is time; C_s is damping ratio of strain velocity; $C(x)$ is the viscous damping coefficient; y is the vertical displacement of the beam and $q(x, t)$ is the loading force per unit length due to the moving vehicle acting on the beam.

To determine the solution of Eq.(13), a modal superposition method is utilized in which the displacement of the beam is expressed as:

$$y(x,t)=\sum_{i=1}^{\infty}A_i(t)\phi(x), \quad (14)$$

where $A_i(t)$ is the time-varying modal amplitude and $\phi(x)$ is the mode shape of the guideway.

The following differential equation for the modal amplitude $A_i(t)$ can be obtained:

$$\ddot{A}_i(t)+2\xi_i\omega_i\dot{A}_i(t)+\omega_i^2A_i(t)=f_i(t), \quad (15)$$

where

$$f_i(t)=\frac{\tilde{P}_i(t)}{\tilde{m}_i},\ \tilde{m}_i=m\int_0^{L_s}\phi_i^2(x)\mathrm{d}x,$$

$$\tilde{P}_i(t)=\int_0^{L_s}\phi_i(x)q(x,t)\mathrm{d}x,\ i=1,2,\cdots,\infty.$$

L_s is the total length of the guideway. The guideway displacement can be determined by Eq.(14) after solving Eq.(15).

Vehicle/guideway interaction

The dynamic interaction between vehicle and guideway occurs when the magnetic force controlled by the control system acts on both vehicle and guideway simultaneously during vehicle's moving on the flexible guideway. The process for deriving the vehicle/guideway interaction involves three steps. The first step is to convert the magnetic forces generated by magnet modules into distributed loading forces along the guideway. The second step is to solve for vibrations of the guideway and the vehicle, which are subjected to the distributed magnetic forces simultaneously. The final step is to obtain the air gap and air gap rate corresponding to each sensor installed on the magnet modules. These data are sent to the control system as feedback signal.

SOLUTION OF DYNAMIC EQUATIONS

The dynamic equations of vehicle/guideway dynamic interaction system described above can be rewritten in the following standard matrix form:

$$\boldsymbol{M}\cdot\boldsymbol{X}''+\boldsymbol{C}\cdot\boldsymbol{X}'+\boldsymbol{K}\cdot\boldsymbol{X}=\boldsymbol{F}, \quad (16)$$

where $\boldsymbol{M}$, $\boldsymbol{C}$, $\boldsymbol{K}$ are the generalized mass, damping and stiffness matrices respectively; $\boldsymbol{X}''$, $\boldsymbol{X}'$, $\boldsymbol{X}$ are the vectors of generalized acceleration, velocity and displacement in vertical direction, respectively; $\boldsymbol{F}$ is the force vector containing the magnetic forces and the generalized modal forces. Due to the vehicle's moving along the guideway, $\boldsymbol{M}$, $\boldsymbol{C}$, $\boldsymbol{K}$, $\boldsymbol{F}$ are all time-variant. So Wilson-θ step-by-step method can be used to solve Eq.(16) and numerical experiments show that with proper control parameters the simulation of an entire process from the vehicle's entering the guideway to the vehicle's leaving the guideway completely can be carried out effectively.

RESULTS AND DISCUSSION

Numerical simulation results

The parameters of TR06 and the guideway have been shown in Tables 1 and 2.

According to the parameters described above, a numerical simulation for dynamic interaction between the vehicle and the guideway has been carried out. In order to obtain stable solutions, the whole simulation process lasts from the vehicle's entering the 1st guideway to the vehicle's leaving the 10th guideway completely and the responses of the 5th guideway are adopted to study the dynamic characteristic of the guideway. Some numerical results are shown in Figs.4 and 5.

Table 1 Parameters of maglev TR06 (Zhao and Zhai, 2002)

Parameters	Values
Carbody mass (kg)	29200
Bogie mass (kg)	8000
Secondary damping (N·s/m)	8.515×10^4
Secondary stiffness (N/m)	1.058×10^4

Table 2 Parameters of the guideway

Parameters	Values
Side span length (m)	37.152
Main span length (m)	71.208
Bending rigidity (N·m^2)	2.256×10^{11}
Mass per unit length (kg/m)	8535.0

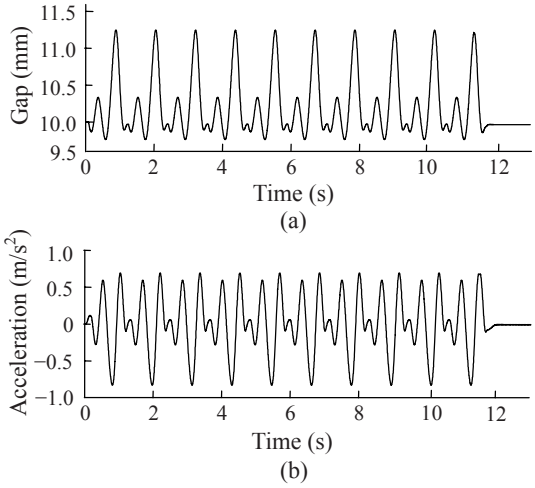

Fig.4 The time history of air gap (a) and acceleration (b) of the first carbody

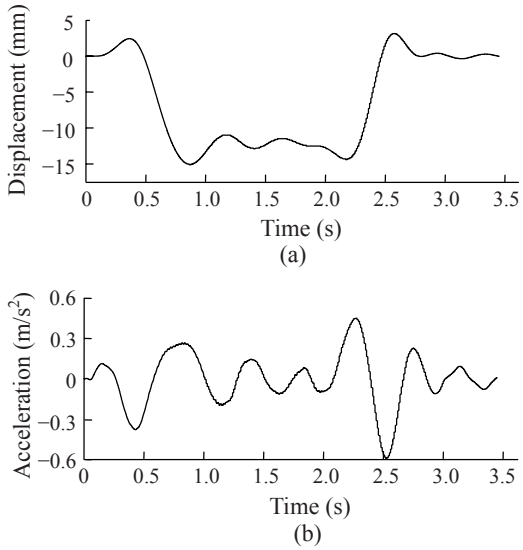

Fig.5 The time history of the displacement (a) and the acceleration (b) of mid-point on the guideway

DISCUSSION

The bending rigidity of the guideway plays an important role in the responses of the guideway. In this paper four kinds of bending rigidity have been proposed. The first one, which acts as the lower limit of bending rigidity, is determined when the main span meets the deformation requirements under static load. The last one, which acts as the upper limit of bending rigidity, is determined when the guideway meets the requirement of $f_1 \geq 1.1v/l$. The other two are selected between the upper limit and lower limit. The contrasts of impact coefficient and acceleration of the guideway are shown in Fig.6.

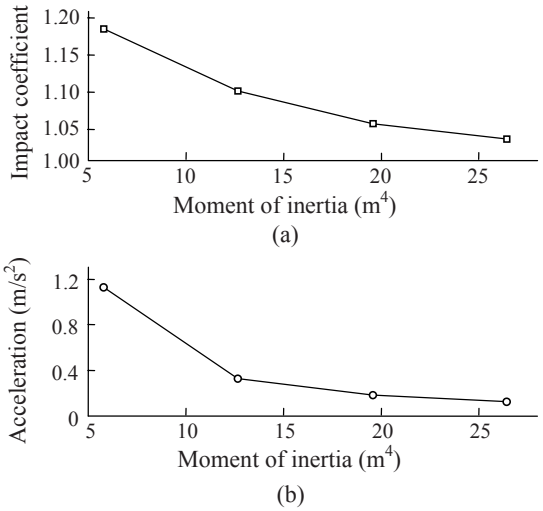

Fig.6 The relationship between the bending rigidity and the impact coefficient (a) and the acceleration (b) of the guideway

Fig.6 indicates that the responses decrease with the increase of bending rigidity. After the bending rigidity increases to certain value, the responses of the guideway decrease slowly and keep at a low level. It is not necessary to adopt the upper limit of the bending rigidity in design.

The relationship between vehicle speed and the responses of the guideway has been shown in Fig.7.

Fig.7 shows that the responses of the guideway increase with the increase of vehicle speed. The impact coefficient increases slowly when vehicle speed is less than 450 km/h and increases greatly when vehicle speed is greater than 450 km/h. The dynamic responses of the guideway increase smoothly within 600 km/h and there is no peak value in this scope studied.

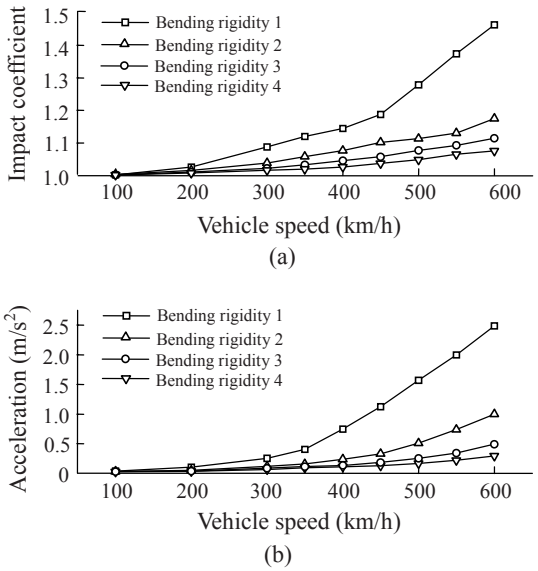

Fig.7 The relationship between vehicle speed and the impact coefficient (a) and the acceleration (b) of the guideway

Span ratio, which is the ratio of l_1 to l_2, is an important factor taken into consideration in design. Under design vehicle speed, the relationship between the span ratio and the responses of the guideway has been shown in Fig.8.

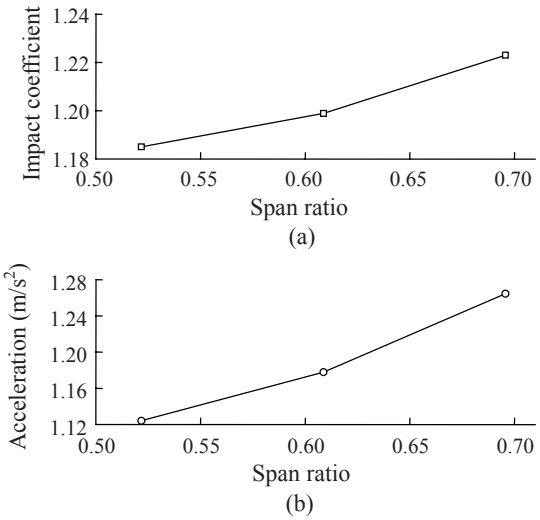

Fig.8 The relationship between the span ratio and the impact coefficient (a) and the acceleration (b) of the guideway

From Fig.8 it can be seen that the dynamic responses of the guideway increase with the increase of the span ratio. Small value of span ratio is given priority when other demands on the guideway have been meet. There is no peak value in the scope studied.

In order to study the comprehensive effect of vehicle speed, side span length and primary frequency of the guideway on the responses of the guideway, the parameter $f_1/(v/l)$ is proposed. The relationship between $f_1/(v/l)$ and the responses of the guideway is shown in Fig.9. In Fig.9, f_1 ranges from 2.46 Hz to 3.82 Hz, v ranges from 100 km/h to 600 km/h and l keeps constant.

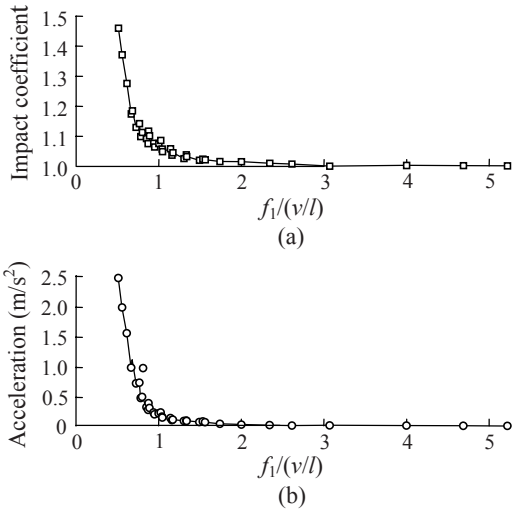

Fig.9 The relationship between $f_1/(v/l)$ and the impact coefficient (a) and the acceleration (b) of the guideway

From Fig.9 it can be seen that the responses of the guideway do not increase or decrease simply with the increase of $f_1/(v/l)$. The viewpoint that the more value of $f_1/(v/l)$ is, the more safe the guideway becomes is incomplete. It can be seen that the responses of the guideway have no obvious change and keep in low level when the value of $f_1/(v/l)$ is greater than 1.5.

The responses of the guideway decrease with the increase of $f_1/(v/l)$ when $f_1/(v/l)$ is around 1.0. But this value is not a critical value and there is no obvious trend towards resonance vibration around this point. So a more definite way is to control the impact coefficient and the acceleration of the guideway in design.

The moving load model and the moving mass model are widely used in studying the vehicle/guideway dynamic interaction in wheels system. Due to the difference between maglev system and wheels system in the way that the interaction generates and acts, it is important to contrast the results from the models mentioned above. The results are shown in Fig.10.

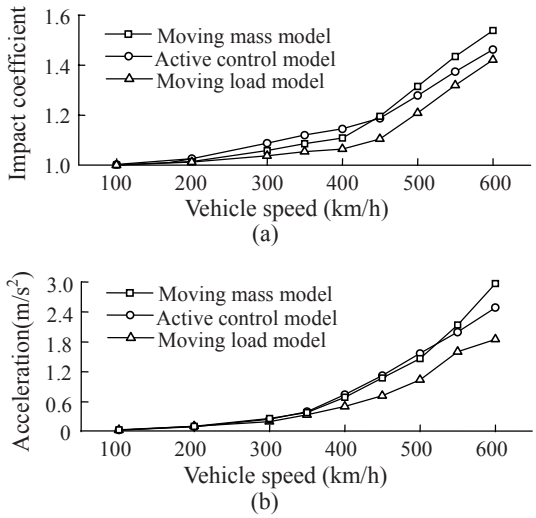

Fig.10 The contrast of the results from the three models
(a) Impact coefficient of the guideway; (b) Acceleration of the guideway

From Fig.10 it can be seen that the results from active control model is the greatest among the three models when vehicle speed is within 400 km/h and that the results from the moving load model are less than others in the scope studied. It can be concluded that it is not exact enough to adopt the moving load model and the moving mass model in the design of high-speed maglev guideway.

CONCLUSION

By calculating and analyzing dynamic responses of the guideway with different parameters, the followings can be concluded:

(1) The dynamic responses of the guideway decrease with the increase of the bending rigidity. As the bending rigidity of the guideway increases to a certain value, the responses of the guideway almost have no change and keep in low level.

(2) The responses of the guideway increase with the increase of vehicle speed and span ratio. There is no peak value within 600 km/h and it is proper to adopt small value of span ratio in guideway design.

(3) It is not the critical point for the responses of the guideway when $f_1/(v/l)$ equals 1.0. The definite way is to control the impact coefficient and the acceleration of the guideway.

(4) It is not exact enough to use the moving load model and the moving mass model in high-speed maglev guideway design.

References

Cai, Y., Chen, S.S., 1996. Control of maglev suspension systems. *Journal of Vibration and Control*, **2**(3):349-368. [doi:10.1177/107754639600200305]

Cai, Y., Chen, S.S., Rote, D.M., Coffey, H.T., 1994. Vehicle guideway interaction for high speed vehicles on a flexible guideway. *Journal of Sound and Vibration*, **175**(5): 625-646. [doi:10.1006/jsvi.1994.1350]

Deng, Y.Q., Liang, H.Q., Luo, S.H., 2006. Static Levitation Stability Simulation and Control of Maglev. Proceedings of the 6th World Congress on Intelligent Control and Automation (WCICA), Dalian, **2**(21-23):6213-6216. [doi:10.1109/WCICA.2006.1714277]

Hong, H.J., Li, J., 2005. The analysis of the equivalence of substituting the controllers with the spring-dampers in maglev system model. *Journal of National University of Defense Technology*, **27**(4):101-105 (in Chinese).

Meisinger, R., 1991. Vehicle-guideway dynamics of a high-speed maglev train. *Chinese Quarterly of Mechanics*, **12**(1):9-20.

Nagurka, M.L., 1995. EMS Maglev Vehicle-Guideway-Controller Model. Proceedings of the American Control Conference, Seattle, p.1167-1168.

Shi, J., Wei, Q.C., Wan, C.F., Deng, Y.S., 2006. Study on dynamic responses of high-speed maglev vehicle/guideway couping system under random irregularity. *Chinese Journal of Theoretical and Applied Mechanics*, **38**(6): 850-857 (in Chinese).

Shi, J., Wei, Q.C., Zhao, Y., 2007. Dynamic simulation of maglev with two degree on flexible guideway. *Journal of System Simulation*, **19**(3):519-523 (in Chinese).

Sinha, P.K., Pechev, A.N., 2004. Nonlinear H_∞ controllers for electromagnetic suspension systems. *IEEE Transactions on Automatic Control*, **49**(4):563-568. [doi:10.1109/TAC.2003.822865]

Wang, H.P., Li, J., 2007. Sub-harmonic resonances of the non-autonomous system with delayed position feedback control. *Acta Physica Sinica*, **56**(5):2504-2516 (in Chinese).

Wang, S.K., 1995. Levitation and Guidance of a Maglev Vehicle Using Optimal Preview Control. Ph.D Thesis, Carnegie Mellon University, Pittsburgh.

Wu, J.J., Zheng, X.J., Zhou, Y.H., 2000. Numerical analysis on dynamic control of five degree of freedom maglev vehicle moving on flexible guideways. *Journal of Sound and Vibration*, **235**(1):43-61. [doi:10.1006/jsvi.1999.2911]

Zhao, C.F., Zhai, W.M., 2002. Maglev vehicle/guideway vertical random response and ride quality. *Vehicle System Dynamics*, **38**(3):185-210. [doi:10.1076/vesd.38.3.185.8289]